

Chapter 6

Design and Analysis of Renewable-Energy-Fed UPQC for Power Quality Improvement



Miska Prasad, Yogesh Kumar Nayak, Rajesh Ranjan Shukla,
Rajagopal Peesapati, and Sudhansu Mehera

Abstract Z-source inverter (ZSI) is a new topology in power converter, especially in DC–AC converter at a very interesting power level. For instance, it only uses a single-stage power converter with the ability of buck–boost characteristic operations. This work introduces a combination of a solar system with unified power quality conditioner (UPQC) based Z-source inverter for reducing the voltage swell and harmonics under the sudden addition of a balanced three-phase nonlinear load. This article additionally proposed another mixture MPPT system, which is the combination of perturbation and observation (P&O) and incremental conductance (InC) methodologies. The modeling and simulation of the proposed UPQC with ZSI has been executed in MATLAB/Simulink for relief of voltage swell and harmonics and the obtained results are contrasted and UPQC with VSI and CSI.

Keywords ZSI · UPQC · Sag · Swell · Solar Energy

6.1 Introduction

These days voltage quality unsettling influences, in particular, voltage droops, and swells represent a genuine danger to the clients (Venkatesh et al. 2011; Alam et al.

M. Prasad (✉)
EEE Department, ACE Engineering College, Hyderabad, India
e-mail: pmiska25@gmail.com

Y. K. Nayak · R. R. Shukla
Electrical Engineering Department, Government College of Engineering, Keonjhar, Odisha, India
e-mail: yogeshnayak_fee@gcekjr.ac.in

R. Peesapati
EEE Department, Raghu Engineering College, Vizag, India
e-mail: rajgopal.peesapati@raghuengcollege.in

S. Mehera
Department of Mechanical Engineering, Government College of Engineering, Keonjhar, Odisha, India
e-mail: sudhansumeher_fme@gcekjr.ac.in

2015). Earlier conventional strategies are proposed to mitigate power quality issues. Yet, of late, to improve the voltage quality, Custom Power Device (CPD) gadgets are utilized. UPQC is the arrangement of shunt associated CPD gadget that is used to limit the voltage hang, swell, and sags in a force dispersion framework (Sundarabalan and Selvi 2015; Sadigh and Smedley 2016; Rahman et al. 2015; Yunfei et al. 2016). Apart from this, the issue of shoot-through or cross-conduction may obliterate the entire IGBT exchanging gadgets. The CSI works as a step-up inverter and the open circuit across the inductor is the main problem. But UPQC with ZSI works as a step-down and step-up inverter (Vodapalli et al. 2015; Reisi et al. 2013; Balamurugan et al. 2013). The voltage infusion ability has both buck and boost capability (Hanif et al. 2011; Zope and Somkuwar 2012; Pilehvar et al. 2015). Because of the nearness of this one-of-a-kind character, it licenses inverters to be worked in the shoot-through mode (Tang et al. 2011; Saravanan et al. 2015; Tajuddin et al. 2015a). Solar energy is one of the most reliable energy sources for renewable energy power generation. It changes the energy from sunlight and converts it using power converters process in order to deliver the generated power to an existing electrical network. As has been known, electrical power consumption increases almost 3.5% every year (Wu et al. 2017). It shows that solar power generation is a very promising electrical generation, especially in a country that receives high sunlight penetration during the day. However, the conventional PV power converters circuit requires two-stage converters (Tajuddin et al. 2015b); the first is to boost the PV voltage to the desired level and then convert the DC input back into AC before it can be fed to the existing electrical grid. Though this configuration is proven to be performing well, it creates lower efficiency, lower reliability, larger in size, more circuitry converters, and produces high power losses as explained in Kannan et al. (2014), Ali (2018) at the output of the converter. As a solution, a Z-source inverter (ZSI) which is based on a passive circuitry process is proposed to overcome the drawbacks of a conventional PV-inverter connection. Currently, ZSI has become an emerging topology in power converter especially in DC-AC converter at a very interesting power level. For instance, it only uses a single-stage power converter with the ability of buck-boost characteristic operations with added features of low ripple input current and high value of voltage gain. These advantages make use of this converter for photovoltaic power generation with high tracking efficiency and achieve better performance (Carrasco and Mancilla-David 2016). Since ZSI is considered a new type of inverter, a lot of research on this area has increased. The focus of the research is to improve the control algorithm, reduce switching schemes, or add a new topology or others (Kannan et al. 2014). However, all of these techniques could not work if the current maximum power point tracking (MPPT) has not been modified to extract more power from the PV for the grid supply (Ahmed and Salam 2016). Consequently, numerous MPPT techniques are reported in the literature (Kandemir et al. 2017; Fathabadi 2016; Alik and Jusoh 2018) and it has been discussed that an emphasis on an improved MPPT can be applied in a Z-source inverter. MPPT approaches can be classified into two categories, which are the conventional and soft computing approaches (Ahmed and Salam 2015). At the moment, the conventional MPPT algorithms such as perturb and observe (P&O) (Umarani and Seyezhai 2016; Tey and Mekhilef 2014), incremental conductance

(InC) (Farhat et al. 2015), hill climbing (HC), etc. have been used intensively in tracking power generated from a solar panel. Several researchers had utilized the Artificial Intelligence techniques such as fuzzy logic control (FLC) (Gheibi et al. 2016), adaptive fuzzy controller (Messalti and Harrag 2015), neural network (NN) (Kermadi and Berkouk 2017) to operate in soft MPPT methods or others names called as soft computing approach. All of them are proven to be very effective in dealing with nonlinear characteristics of solar cells based on the PV I–V curve characteristics.

6.2 PV UPQC with VSI, CSI, and ZSI

Solar photovoltaic UPQC with VSI, CSI, and ZSI is highlighted in Figs. 6.1, 6.2 and 6.3. The DC-connection of both dynamic force channels is associated with a typical DC-interface capacitor for a situation of VSI-UPQC, regular DC-interface inductance for a situation of CSI-UPQC, and both if there should arise an occurrence of ZSI-UPQC. The arrangement gadget of the UPQCs, otherwise called an arrangement dynamic force channel, keeps the customer load end voltages inhumane toward the inventory voltage quality issues like hang/swell, floods, vacillations, and unbalance. The shunt gadget of the UPQCs, otherwise called a shunt dynamic force channel, gives responsive force remuneration, load adjusting, and disposal of sounds (Fig. 6.2).

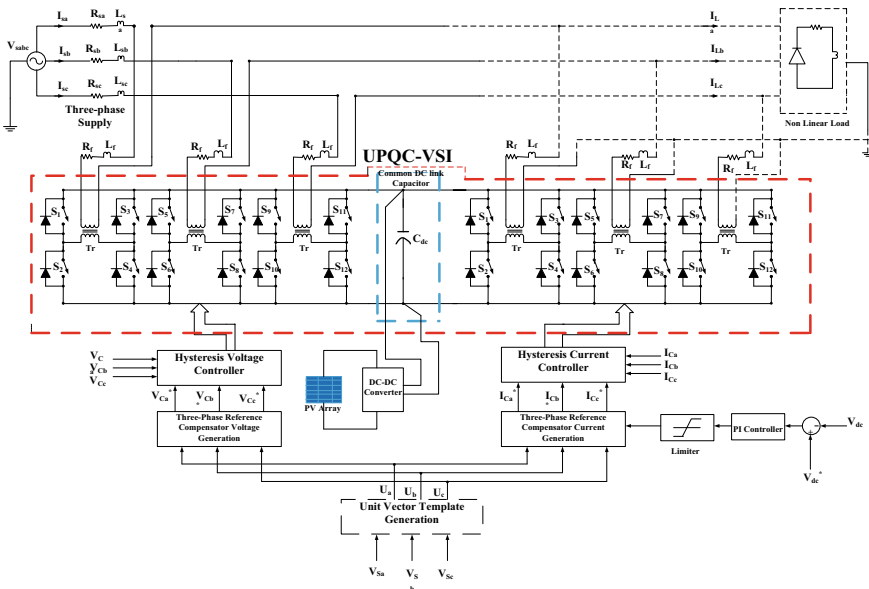


Fig. 6.1 UPQC with VSI

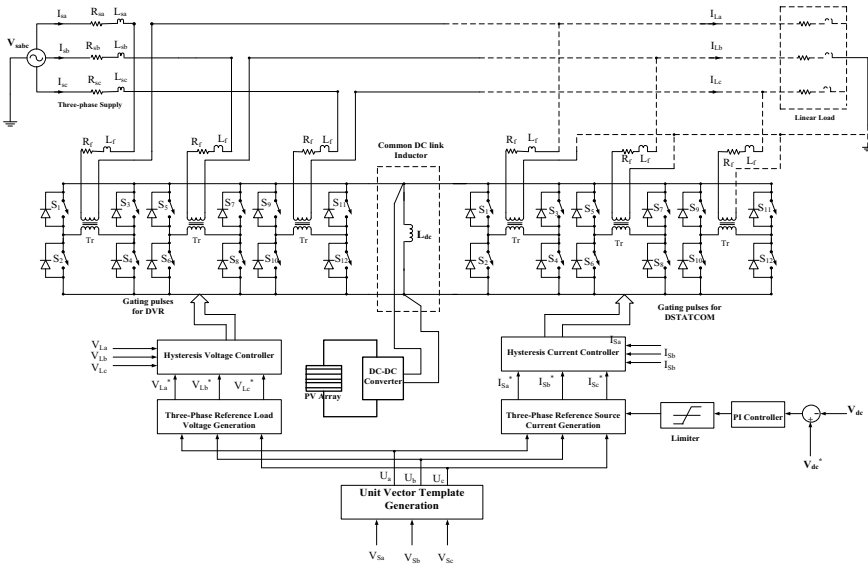


Fig. 6.2 UPQC with CSI

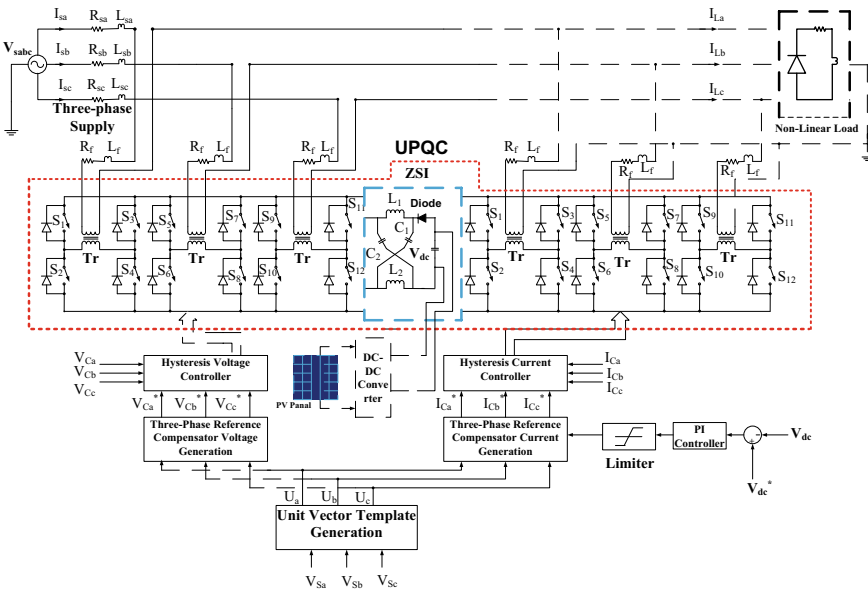


Fig. 6.3 UPQC with ZSI

6.3 Working States of ZSI

The action of ZSI can be finished after three modes such as active mode, zero-state mode, and shoot-through (ST) mode as shown in Fig. 6.4(a-c). The parameters in Figs. 6.1–6.3 are highlighted in Table 6.1.

Let us consider impedance network elements have a similar value ($L_1 = L_2 = L$ and $C_1 = C_2 = C$).

Hence, the voltage relation of ZSI is (Hanif et al. 2011; Pilehvar et al. 2015)

$$\left. \begin{aligned} V_{L1} &= V_{L2} = V_L \\ V_{C1} &= V_{C2} = V_C \end{aligned} \right\} \quad (6.1)$$

where t_0 is the range of shoot-through mode (Hanif et al. 2011; Pilehvar et al. 2015).

$$\left. \begin{aligned} V_L &= V_C \\ V_{diode} &= 2V_C \\ V_{dc-1} &= 0 \text{ (because shoot-through)} \end{aligned} \right\} \quad (6.2)$$

where t_1 is the range of normal and zero-state mode (Hanif et al. 2011; Pilehvar et al. 2015).

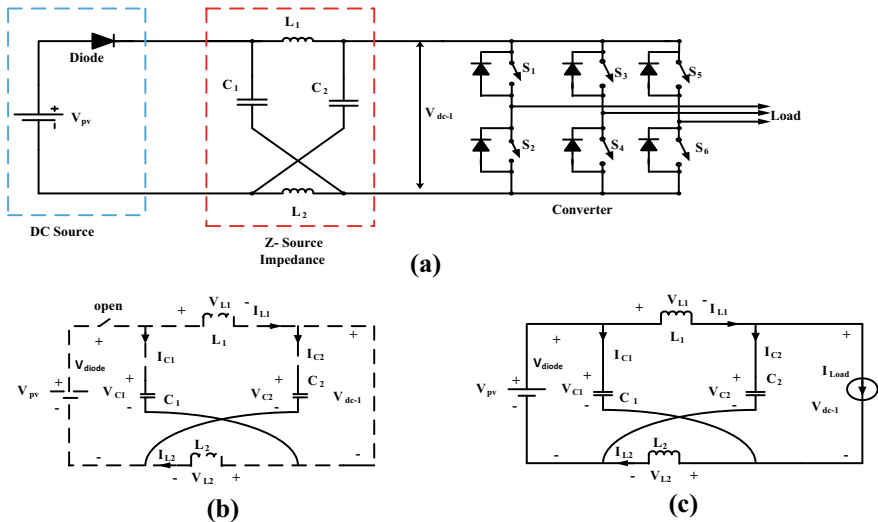


Fig. 6.4 a ZSI, b ST, and c active and zero mode

Table 6.1 Value of elements in Figs. 6.1–6.3

| Parameter | Value |
|---|--------------|
| Solar photovoltaic output voltage (V_{PV}) | 35.5 V |
| ZSI Inductance ($L1 = L2$) | 0.6 mH |
| ZSI Capacitor ($C1 = C2$) | 0.05 μ F |
| Peak DC-link voltage Vdc-1 (during shoot-through mode) | 0 V |
| Vdc-1 (during active and null mode) | 300 V |
| Voltage across capacitor (V_C) | 167.75 V |
| Voltage across inductor (V_L) | –132.25 V |
| Modulation index (M) | 0.5 |
| Shoot-through duty ratio (D) | 0.49 |
| Shoot-through time per cycle (t_0) | 9.83 μ s |
| Non-shoot-through time per cycle (t_1) | 12.8 μ s |
| Total Switching Period (t) | 0.02 ms |
| Average current through inductor ($I_{L,Avg}$) | 4.28 A |
| Maximum inductor current ($I_{L,Max}$) | 5.56 A |
| Minimum inductor current ($I_{L,Min}$) | 2.99 A |
| Switching frequency (fs) | 50 kHz |

$$\left. \begin{aligned} V_L &\neq V_C \\ V_{diode} &= V_{PV} = V_L + V_C \\ V_L &= V_{PV} - V_C = V_C - V_{dc-1} \\ V_{dc-1} &= V_C - V_L = 2V_C - V_{PV} \end{aligned} \right\} \quad (6.3)$$

where V_{pv} is solar photovoltaic output voltage.

At switching period t, the mean voltage of the inductor during steady state is zero ($V_{L,Avg}$) (Hanif et al. 2011; Pilehvar et al. 2015).

$$V_{L,Avg} = V_C * t_0 + (V_{PV} - V_C) * t_1 = 0$$

$$V_C = V_{PV} \left(\frac{t_1}{t_1 - t_0} \right) \quad (6.4)$$

Normal DC-connect voltage of inverter (Vdc-1).

$V_{dc-1} = t_0 * 0 + t_1(2V_C - V_{PV})$ using Eq. (6.4)

$$V_{dc-1} = \left(\frac{t_1}{t_1 - t_0} \right) V_{PV} = V_C \quad (6.5)$$

Maximum DC-link voltage

$$\hat{V}_{dc-1} = (V_C - V_L) = V_C - (V_{PV} - V_C)$$

$$\hat{V}_{dc-1} = (2V_C - V_{PV}) \quad (6.6)$$

$$\hat{V}_{dc-1} = BV_{PV} \quad (6.7)$$

$$B = \left(\frac{t}{t_1 - t_0} \right) = \frac{1}{1 - \left(\frac{2t_0}{t} \right)} \geq 1, \quad t = t_0 + t_1 \quad (6.8)$$

The converter output voltage can be calculated as (Hanif et al. 2011; Pilehvar et al. 2015)

$$V_{AC} = \frac{M V_{dc-1}}{2} = \left(\frac{MBV_{PV}}{2} \right) \quad (6.9)$$

Voltage across the capacitor (Hanif et al. 2011; Pilehvar et al. 2015).

From Eq. (6.4), we have

$$V_C = \left(\frac{t_1}{t_1 - t_0} \right) V_{PV}$$

$$V_C = \left(\frac{t_1}{t} \right) \left(\frac{t}{t_1 - t_0} \right) V_{PV} \quad (6.10)$$

$$V_C = \left(\frac{1 - (t_0/t)}{1 - (2t_0/t)} \right) V_{PV}$$

$$V_C = \frac{B+1}{2B} * B * V_{PV} = \left(\frac{B+1}{2} \right) V_{PV} \quad (6.11)$$

6.4 Modulation Algorithm With Timing Diagram of the Proposed Z-Source Inverter

Figure 6.5 shows the structure and Table 6.2 lists the 83 switching states of the proposed Z-Source inverter, which includes 40 active states, 2 null states, and 41 shoot-through states.

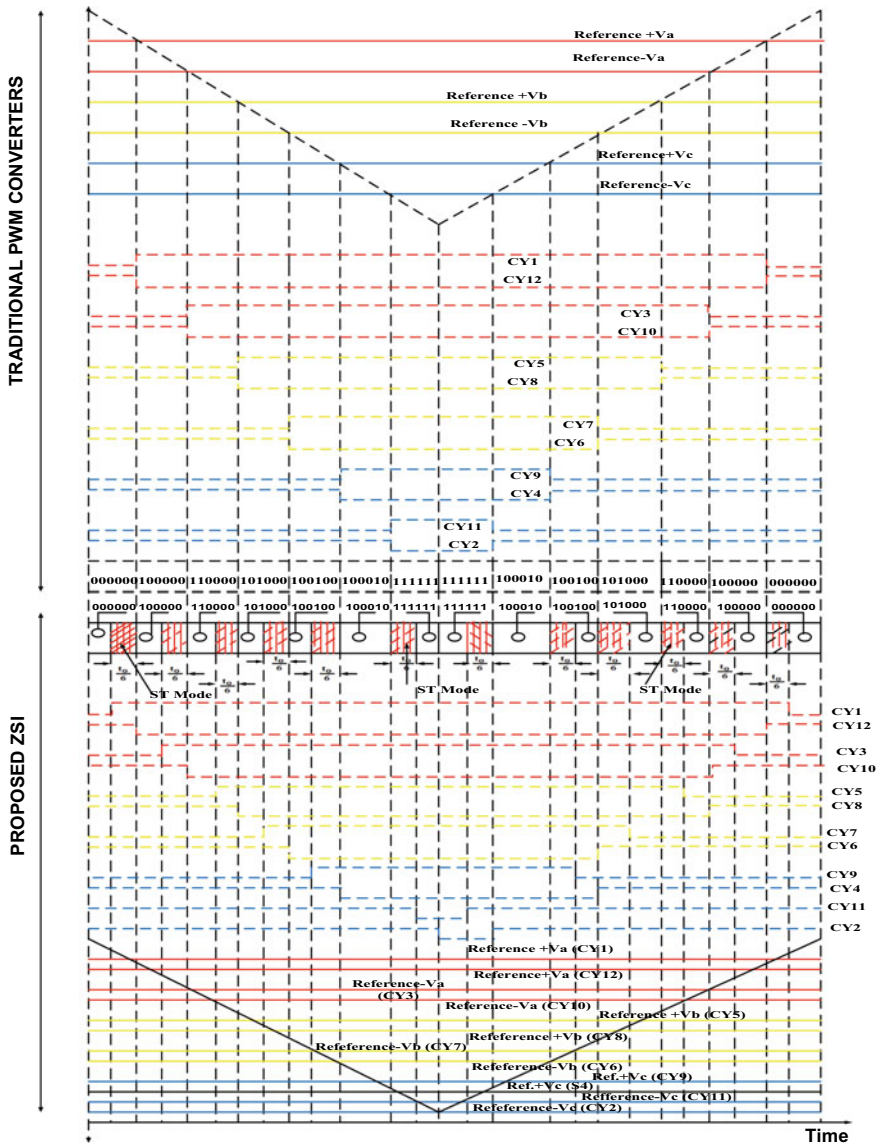


Fig 6.5 Z-Source Inverter Modulation

6.5 Proposed Hybrid Technique

The most regularly utilized MPPT regulators are P&O (Umarani and Seyezhai 2016; Tey and Mekhilef 2014) and the InC (Farhat et al. 2015) MPPT regulator. These regulators likewise have not many downsides which now and again could be an issue

Table 6.2 Switching States of the proposed ZSI (!CY represents complement of SX, where Y = 1, 3, 5, 7, 9, or 11)

| State{100,000}(finite) | C1 | C12 | C3 | C10 | C5 | C8 | C7 | C6 | C9 | C4 | C11 | C2 |
|------------------------|----|-----|----|-----|----|----|----|----|----|----|-----|----|
| State{110,000}(finite) | 1 | 0 | 0 | 1 | 0 | 1 | 0 | 1 | 0 | 1 | 0 | 1 |
| State{101,000}(finite) | 1 | 0 | 1 | 0 | 0 | 1 | 0 | 1 | 0 | 1 | 0 | 1 |
| State{100,100}(finite) | 1 | 0 | 0 | 1 | 1 | 0 | 0 | 1 | 0 | 1 | 0 | 1 |
| State{100,010}(finite) | 1 | 0 | 0 | 1 | 0 | 1 | 0 | 1 | 1 | 0 | 0 | 1 |
| State{100,001}(finite) | 1 | 0 | 0 | 1 | 0 | 1 | 0 | 1 | 0 | 1 | 1 | 0 |
| State{010,000} finite | 0 | 1 | 1 | 0 | 0 | 1 | 0 | 1 | 0 | 1 | 0 | 1 |
| State{011,000} finite | 0 | 1 | 1 | 0 | 1 | 0 | 0 | 1 | 0 | 1 | 0 | 1 |
| State{010,100} finite | 0 | 1 | 1 | 0 | 0 | 1 | 1 | 0 | 0 | 1 | 0 | 1 |
| State {010,010} finite | 0 | 1 | 1 | 0 | 0 | 1 | 0 | 1 | 1 | 0 | 0 | 1 |
| State {010,001} finite | 0 | 1 | 1 | 0 | 0 | 1 | 0 | 1 | 0 | 1 | 1 | 0 |
| State {001,000} finite | 0 | 1 | 0 | 1 | 1 | 0 | 0 | 1 | 0 | 1 | 0 | 1 |
| State {001,100} finite | 0 | 1 | 0 | 1 | 1 | 0 | 1 | 0 | 0 | 1 | 0 | 1 |
| State {001,010} finite | 0 | 1 | 0 | 1 | 1 | 0 | 0 | 1 | 1 | 0 | 0 | 1 |
| State {001,001} finite | 0 | 1 | 0 | 1 | 1 | 0 | 0 | 1 | 0 | 1 | 1 | 0 |
| State {000,100} finite | 0 | 1 | 0 | 1 | 0 | 1 | 1 | 0 | 0 | 1 | 0 | 1 |
| State {000,110} finite | 0 | 1 | 0 | 1 | 0 | 1 | 1 | 0 | 1 | 0 | 0 | 1 |
| State {000,101} finite | 0 | 1 | 0 | 1 | 0 | 1 | 1 | 0 | 0 | 1 | 1 | 0 |
| State {000,010} finite | 0 | 1 | 0 | 1 | 0 | 1 | 0 | 1 | 1 | 0 | 0 | 1 |
| State {000,011} finite | 0 | 1 | 0 | 1 | 0 | 1 | 0 | 1 | 1 | 0 | 1 | 0 |
| State {111,000} finite | 1 | 0 | 1 | 0 | 1 | 0 | 0 | 1 | 0 | 1 | 0 | 1 |
| State {110,100} finite | 1 | 0 | 1 | 0 | 0 | 1 | 1 | 0 | 0 | 1 | 0 | 1 |
| State {110,010} finite | 1 | 0 | 1 | 0 | 0 | 1 | 0 | 1 | 1 | 0 | 0 | 1 |
| State {110,001} finite | 1 | 0 | 1 | 0 | 0 | 1 | 0 | 1 | 0 | 1 | 1 | 0 |
| State {011,100} finite | 0 | 1 | 1 | 0 | 1 | 0 | 1 | 0 | 0 | 1 | 0 | 1 |
| State {011,010} finite | 0 | 1 | 1 | 0 | 1 | 0 | 0 | 1 | 1 | 0 | 0 | 1 |
| State {011,001} finite | 0 | 1 | 1 | 0 | 1 | 0 | 0 | 1 | 0 | 1 | 1 | 0 |
| State {001,110} finite | 0 | 1 | 0 | 1 | 1 | 0 | 1 | 0 | 1 | 0 | 0 | 1 |
| State {001,101} finite | 0 | 1 | 0 | 1 | 1 | 0 | 1 | 0 | 0 | 1 | 1 | 0 |
| State {000,111} finite | 0 | 1 | 0 | 1 | 0 | 1 | 1 | 0 | 1 | 0 | 1 | 0 |
| State {100,011} finite | 1 | 0 | 0 | 1 | 0 | 1 | 0 | 1 | 1 | 0 | 1 | 0 |
| State {111,100} finite | 1 | 0 | 1 | 0 | 1 | 0 | 1 | 0 | 0 | 1 | 0 | 1 |
| State {111,010} finite | 1 | 0 | 1 | 0 | 1 | 0 | 0 | 1 | 1 | 0 | 0 | 1 |
| State {111,001} finite | 1 | 0 | 1 | 0 | 1 | 0 | 0 | 1 | 0 | 1 | 1 | 0 |
| State {011,110} finite | 0 | 1 | 1 | 0 | 1 | 0 | 1 | 0 | 1 | 0 | 0 | 1 |
| State {011,101} finite | 0 | 1 | 1 | 0 | 1 | 0 | 1 | 1 | 0 | 1 | 1 | 0 |

(continued)

Table 6.2 (continued)

| State{100,000}(finite) | C1 | C12 | C3 | C10 | C5 | C8 | C7 | C6 | C9 | C4 | C11 | C2 |
|-------------------------|----|-----|----|-----|----|-----|----|-----|----|-----|-----|------|
| State {001,111} finite | 0 | 1 | 0 | 1 | 1 | 0 | 1 | 0 | 1 | 0 | 1 | 0 |
| State {100,111} finite | 1 | 0 | 0 | 1 | 0 | 1 | 1 | 0 | 1 | 0 | 1 | 0 |
| State {111,110} finite | 1 | 0 | 1 | 0 | 1 | 0 | 1 | 0 | 1 | 0 | 0 | 1 |
| State {011,111} finite | 0 | 1 | 1 | 0 | 1 | 0 | 1 | 0 | 1 | 0 | 1 | 0 |
| Null {000,000} (0 V) | 0 | 1 | 0 | 1 | 0 | 1 | 0 | 1 | 0 | 1 | 0 | 1 |
| Null{111,111} (0 V) | 1 | 0 | 1 | 0 | 1 | 0 | 1 | 0 | 1 | 0 | 1 | 0 |
| Shoot-through F1 (0 V) | 1 | 1 | C3 | !C3 | C5 | !C5 | C7 | !C7 | C9 | !C9 | C11 | !C11 |
| Shoot-through F2 (0 V) | C1 | !C1 | 1 | 1 | C5 | !C5 | C7 | !C7 | C9 | !C9 | C11 | !C11 |
| Shoot-through F3 (0 V) | C1 | !C1 | C3 | !C3 | 1 | 1 | C7 | !C7 | C9 | !C9 | C11 | !C11 |
| Shoot-through F4 (0 V) | C1 | !C1 | C3 | !C3 | C5 | !C5 | 1 | 1 | C9 | !C9 | C11 | !C11 |
| Shoot-through F5 (0 V) | C1 | !C1 | C3 | !C3 | C5 | !C5 | C7 | !C7 | 1 | 1 | C11 | !C11 |
| Shoot-through F6 (0 V) | C1 | !C1 | C3 | !C3 | C5 | !C5 | C7 | !C7 | C9 | !C9 | 1 | 1 |
| Shoot-through F7 (0 V) | 1 | 1 | 1 | 1 | C5 | !C5 | C7 | !C7 | C9 | !C9 | C11 | !C11 |
| Shoot-through F8 (0 V) | 1 | 1 | C3 | !C3 | 1 | 1 | C7 | !C7 | C9 | !C9 | C11 | !C11 |
| Shoot-through F9 (0 V) | 1 | 1 | C3 | !C3 | C5 | !C5 | 1 | 1 | C9 | !C9 | C11 | !C11 |
| Shoot-through F10(0 V) | 1 | 1 | C3 | !C3 | C5 | !C5 | C7 | !C7 | 1 | 1 | C11 | !C11 |
| Shoot-through F11(0 V) | 1 | 1 | C3 | !C3 | C5 | !C5 | C7 | !C7 | C9 | !C9 | 1 | 1 |
| Shoot-through F12(0 V) | C1 | !C1 | 1 | 1 | 1 | 1 | C7 | !C7 | C9 | !C9 | C11 | !C11 |
| Shoot-through F13(0 V) | C1 | !C1 | 1 | 1 | C5 | !C5 | 1 | 1 | C9 | !C9 | C11 | !C11 |
| Shoot-through F14 (0 V) | C1 | !C1 | 1 | 1 | C5 | !C5 | C7 | !C7 | 1 | 1 | C11 | !C11 |
| Shoot-through F15(0 V) | C1 | !C1 | 1 | 1 | C5 | !C5 | C7 | !C7 | C9 | !C9 | 1 | 1 |
| Shoot-through F16(0 V) | C1 | !C1 | C3 | !C3 | 1 | 1 | 1 | 1 | C9 | !C9 | C11 | !C11 |
| Shoot-through F17(0 V) | C1 | !C1 | C3 | !C3 | 1 | 1 | C7 | !C7 | 1 | 1 | C11 | !C11 |
| Shoot-through F18(0 V) | C1 | !C1 | C3 | !C3 | 1 | 1 | C7 | !C7 | C9 | !C9 | 1 | 1 |
| Shoot-through F19(0 V) | C1 | !C1 | C3 | !C3 | C5 | !C5 | 1 | 1 | 1 | 1 | C11 | !C11 |
| Shoot-through F20(0 V) | C1 | !C1 | C3 | !C3 | C5 | !C5 | 1 | 1 | C9 | !C9 | 1 | 1 |
| Shoot-through F21(0 V) | C1 | !C1 | C3 | !C3 | C5 | !C5 | C7 | !C7 | 1 | 1 | 1 | 1 |
| Shoot-through F22(0 V) | 1 | 1 | 1 | 1 | 1 | 1 | C7 | !C7 | C9 | !C9 | C11 | !C11 |
| Shoot-through F23(0 V) | 1 | 1 | 1 | 1 | C5 | !C5 | 1 | 1 | C9 | !C9 | C11 | !C11 |
| Shoot-through F24(0 V) | 1 | 1 | 1 | 1 | C5 | !C5 | C7 | !C7 | 1 | 1 | C11 | !C11 |
| Shoot-through F25(0 V) | 1 | 1 | 1 | 1 | C5 | !C5 | C7 | !C7 | C9 | !C9 | 1 | 1 |
| Shoot-through F26(0 V) | C1 | !C1 | 1 | 1 | 1 | 1 | 1 | 1 | C9 | !C9 | C11 | !C11 |
| Shoot-through F27(0 V) | C1 | !C1 | 1 | 1 | 1 | 1 | C7 | !C7 | 1 | 1 | C11 | !C11 |
| Shoot-through F28(0 V) | C1 | !C1 | 1 | 1 | 1 | 1 | C7 | !C7 | C9 | !C9 | 1 | 1 |
| Shoot-through F29(0 V) | C1 | !C1 | C3 | !C3 | 1 | 1 | 1 | 1 | 1 | 1 | C11 | !C11 |

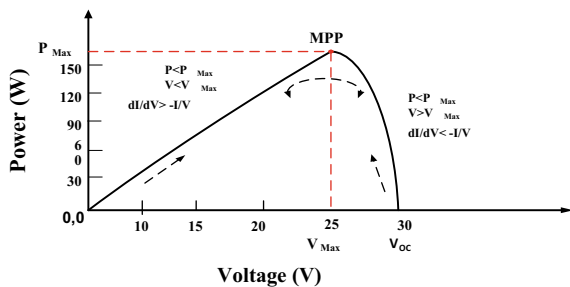
(continued)

Table 6.2 (continued)

| State{100,000}(finite) | C1 | C12 | C3 | C10 | C5 | C8 | C7 | C6 | C9 | C4 | C11 | C2 |
|------------------------|----|-----|----|-----|----|-----|----|-----|----|-----|-----|------|
| Shoot-through F30(0 V) | C1 | !C1 | C3 | !C3 | 1 | 1 | 1 | 1 | C9 | !C9 | 1 | 1 |
| Shoot-through F31(0 V) | C1 | !C1 | C3 | !C3 | C5 | !C5 | 1 | 1 | 1 | 1 | 1 | 1 |
| Shoot-through F32(0 V) | 1 | 1 | 1 | 1 | 1 | 1 | 1 | 1 | C9 | !C9 | C11 | !C11 |
| Shoot-through F33(0 V) | 1 | 1 | 1 | 1 | 1 | 1 | C7 | !C7 | 1 | 1 | C11 | !C11 |
| Shoot-through F34(0 V) | 1 | 1 | 1 | 1 | 1 | 1 | C7 | !C7 | C9 | !C9 | 1 | 1 |
| Shoot-through F35(0 V) | C1 | !C1 | 1 | 1 | 1 | 1 | 1 | 1 | 1 | 1 | C11 | !C11 |
| Shoot-through F36(0 V) | C1 | !C1 | 1 | 1 | 1 | 1 | 1 | 1 | C9 | !C9 | 1 | 1 |
| Shoot-through F37(0 V) | C1 | !C1 | C3 | !C3 | 1 | 1 | 1 | 1 | 1 | 1 | 1 | 1 |
| Shoot-through F38(0 V) | 1 | 1 | 1 | 1 | 1 | 1 | 1 | 1 | 1 | 1 | C11 | !C11 |
| Shoot-through F39(0 V) | 1 | 1 | 1 | 1 | 1 | 1 | 1 | 1 | C9 | !C9 | 1 | 1 |
| Shoot-through F40(0 V) | C1 | !C1 | 1 | 1 | 1 | 1 | 1 | 1 | 1 | 1 | 1 | 1 |
| Shoot-through F41(0 V) | 1 | 1 | 1 | 1 | 1 | 1 | 1 | 1 | 1 | 1 | 1 | 1 |

while following the force from PV modules. Henceforth, another crossbreed MPPT regulator is proposed in this paper that disposes of the defeats of both P&O and INC MPPT regulators. The proposed MPPT regulator likewise expects to join the advantages of both the existing MPPT regulators. The cross-breed MPPT method is proposed to dispose of the constraints of both P&O and InC procedures as portrayed in Fig. 6.6. The principal focus of this proposed method is to gain the merge benefits of both and perception and steady conductance techniques. It estimates voltage and current from the sun-oriented PV board and computes yield power. Subsequent to ascertaining the yield power, the proposed procedure stores power, estimated voltage, and estimated current in a brief memory for examination. Presently, it contrasts the force and the past estimation of force by finding the adjustment in power. The proposed computation checks whether $\Delta I/\Delta V$ is more noticeable than, not actually, or identical to $-I/V$ and makes its decision whether to augmentation or reduction the terminal voltage.

Fig. 6.6 Hybrid strategy



6.6 Results and Discussion

To show the usefulness of the PV dealt with VSI-, CSI-, and ZSI-based UPQCs with its connected UVT control strategy and the power circuit given in Figs. 6.1–6.3 have been set up with MATLAB/Simulink programming. The PV exhibit with chopper gives a more prominent yield voltage. Figure 6.7 shows the PV cluster voltage without and with a chopper. Figure 6.8a–c highlights that the force yield of the proposed half and half strategy is more viable in separating the most extreme force point (MPP = 152 W) from a sun-based PV framework contrasted with the greatest force point (MPP = 151 W) for a situation of P&O procedure and greatest force point (MPP = 152.58 W) for a situation of gradual conductance technique. The primary goal of this part is to assess the presentation of the PV took care of UPQC with ZSI in examination with that of PV took care of UPQC with VSI and UPQC with CSI for the easing of force quality occasions, for example, voltage swells and sounds in supply current just as burden voltage.

Fig. 6.7 Solar system output voltage with and without a chopper

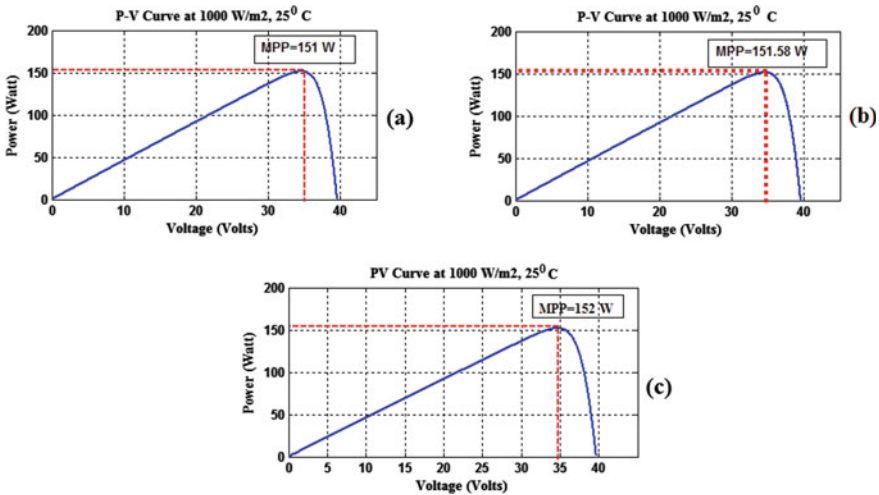
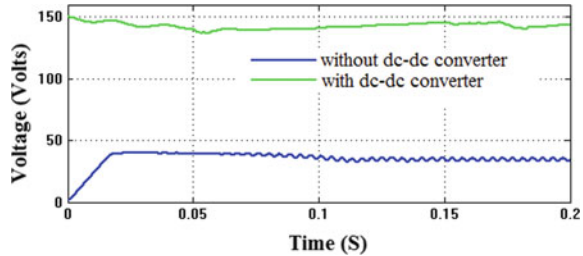


Fig. 6.8 a P&O, b InC, and c the proposed hybrid scheme

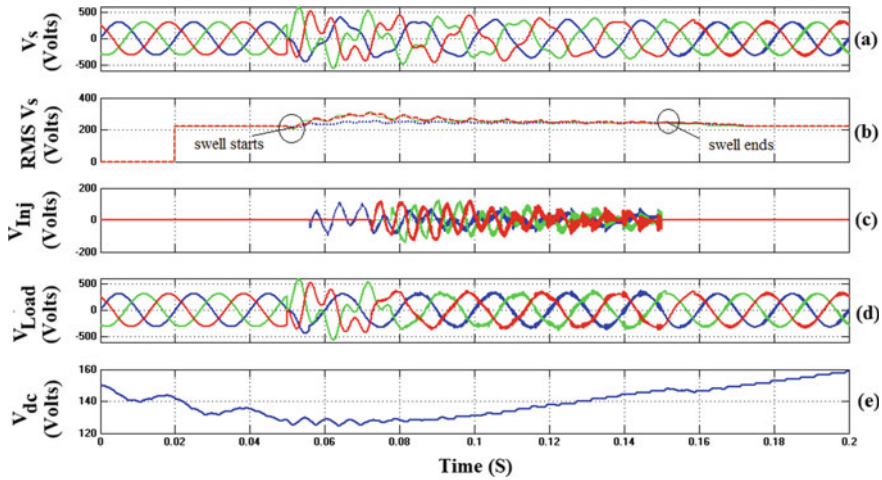


Fig. 6.9 Swell alleviation by UPQC with VSI

6.6.1 Swell Alleviation by UPQC with VSI

The presentation of UPQC with VSI is featured in Fig. 6.9a–e for limiting the voltage enlarge. A voltage swell of size 20% is noted as displayed in Fig. 6.9a–b. To limit this issue, sun-powered photovoltaic-based UPQC with VSI comes right into it and infuses missing voltage as displayed in Fig. 6.9c. The infused voltage is added to supply voltage and, consequently, the load voltage is liberated from voltage expansion as displayed in Fig. 6.9d. The conduct of DC-connect voltage during voltage expansion occasion uncovered in Fig. 6.9e.

6.6.2 Swell Alleviation by UPQC with CSI

A swell of size 20% saw as displayed in Fig. 6.10a–b. To restrict this voltage enlargement, sun-based photovoltaic-based UPQC with CSI is related and produces the required measure voltage as shown in Fig. 6.10c. To restrict this issue, the solar system connected UPQC with CSI comes right into it and injects the required voltage as featured in Fig. 6.10c. The infused voltage is added to supply voltage and, consequently, the load voltage is liberated from voltage enlarge as displayed in Fig. 6.10d. The conduct of inductor current during voltage growth occasion is uncovered in Fig. 6.10e.

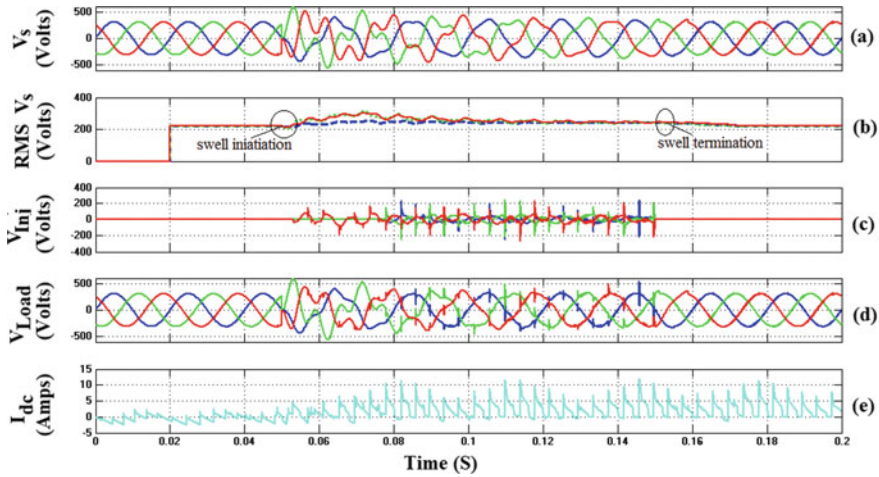


Fig. 6.10 Swell alleviation by UPQC with CSI

6.6.3 Swell Alleviation by UPQC with ZSI

The strength of UPQC with ZSI is featured in Fig. 6.11a–f for alleviation of voltage enlargement. Without UPQC, a voltage swell of size 20% is noted as displayed in Fig. 6.11a–b. To decrease the impact of voltage enlarge, the solar system connected UPQC with ZSI comes right into it and infuses the required voltage as featured in Fig. 6.11c. The UPQC infused voltage is added to source voltage and, consequently, the load voltage is liberated from voltage expansion as displayed in Fig. 6.11d. The

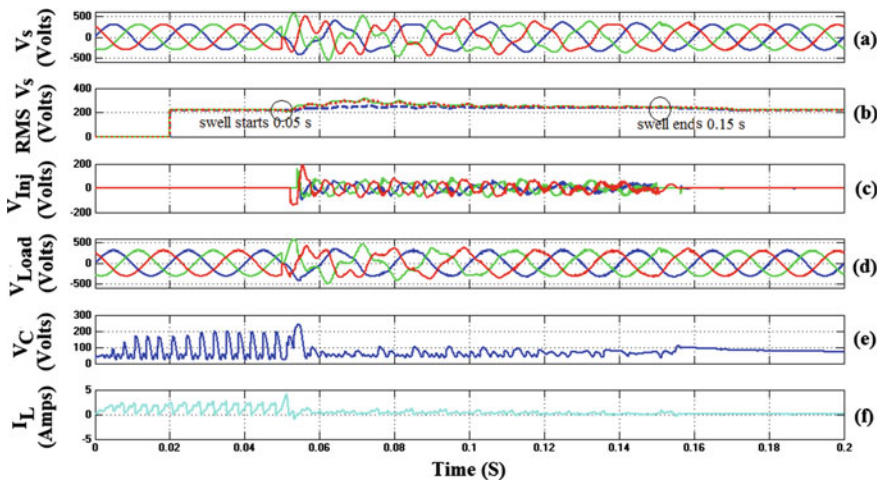


Fig. 6.11 Response of UPQC with ZSI

conduct of DC-interface voltage and inductor current during voltage growth occasion uncovered in Fig. 6.11e and f.

Changed and uncompensated burden voltages under voltage swell conditions are depicted in Fig. 6.12. From the outset, when UPQC with VSI, CSI, and ZSI is not related to the structure, the system encounters a voltage swell of a degree of 20% (60 V) of the load voltage. During voltage grow event UPQC with VSI implants the voltage of 120 V, UPQC with CSI injects the voltage of 200 V and UPQC with ZSI imbues the voltage of 75 V as exhibited in Fig. 6.12a. The PV connected UPQC with ZSI shows the preferable display over make the reasonable proportion of imbued voltage appeared differently in relation to UPQC with VSI and UPQC with CSI. Appropriately, load voltage gets sinusoidal as exhibited in Fig. 6.12b.

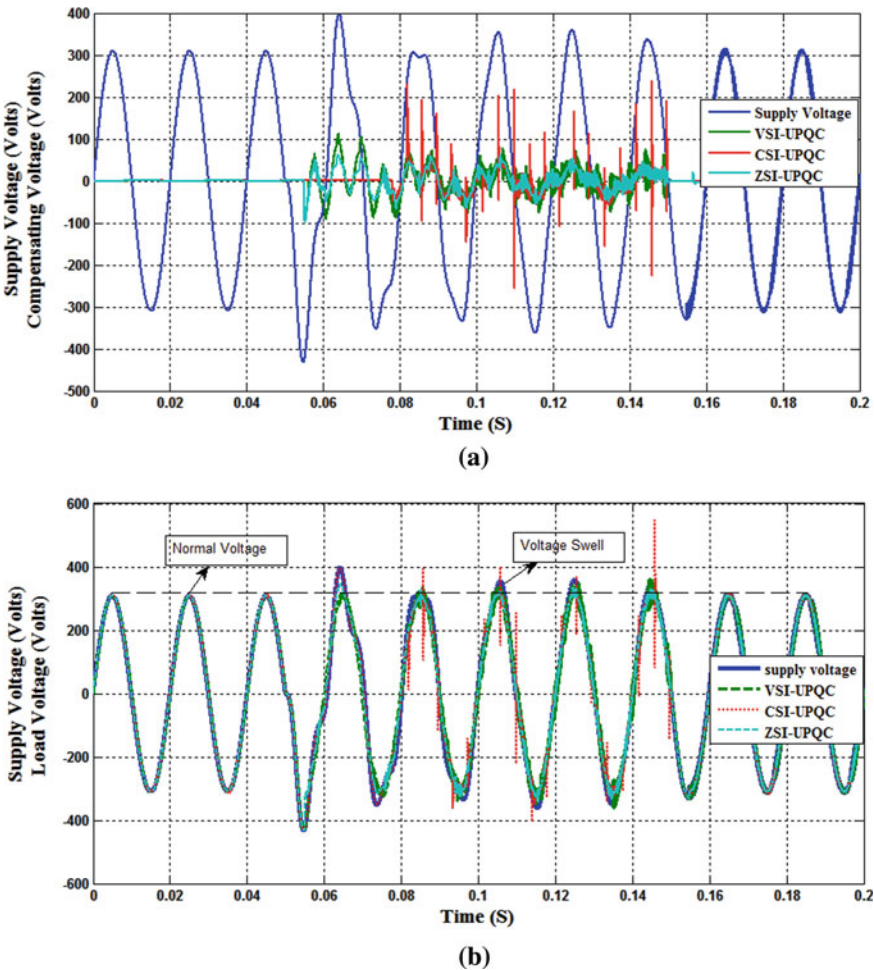


Fig. 6.12 a Injected voltages and b load voltages

Table 6.3 Supply current harmonics THD_i of VSI, CSI, and ZSI UPQCs

| Without UPQCs | UPQC-VSI | | UPQC-CSI | | UPQC-ZSI | |
|---------------|---------------|-------------------------------------|---------------|-------------------------------------|---------------|-------------------------------------|
| | With UPQC-VSI | Improvement in THD _i (%) | With UPQC-CSI | Improvement in THD _i (%) | With UPQC-ZSI | Improvement in THD _i (%) |
| 7.28 | 1.67 | 77.06 | 1.66 | 77.20 | 1.60 | 78.02 |

Table 6.4 Load voltage harmonics THD_s of VSI, CSI, and ZSI UPQCs

| Without UPQCs | UPQC-VSI | | UPQC-CSI | | UPQC-ZSI | |
|---------------|---------------|-------------------------------------|---------------|-------------------------------------|---------------|-------------------------------------|
| | With UPQC-VSI | Improvement in THD _s (%) | With UPQC-CSI | Improvement in THD _s (%) | With UPQC-ZSI | Improvement in THD _s (%) |
| 18.62 | 2.31 | 87.60 | 2.48 | 86.68 | 1.48 | 92.05 |

The exhibition of supply current as well as load harmonics filtering of PV took care of UPQCs during load exchanging condition as shown in Tables 6.3–6.4. During load exchanging, the source current THD_i before pay is discovered to be 7.97%, while THD_i of the source current after remuneration is discovered to be 0.72% in the presence of UPQC-VSI with a 90.96% decrease in THD_i, 0.83% if there should arise an occurrence of UPQC-CSI with an 89.58% decrease in THD_i and 0.72% in the presence of ZSI-UPQC with a 90.96% decrease in THD_i individually as demonstrated in Table 6.3. In this way, VSI-UPQC and CSI-UPQC are decreasing a lesser measure of THD_i in contrast with UPQC-ZSI.

Table 6.4 summed up the THD_v correlation of PV connected UPQC with VSI, CSI, and ZSI during load exchanging. From table 6.4, it is featured that THD_v of load voltage before remuneration is recorded to be 18.62%, and the THD_v of load voltage after pay is discovered to be 2.31% if there should arise an occurrence of UPQC with VSI, 2.48% in presence of UPQC with CSI and 1.48% in presence of ZSI-UPQC. Along these lines, an 87.60% decrease in THD_v has been accomplished utilizing UPQC with ZSI contrasted with an 86.68% decrease in THD_v of UPQC-VSI and 92.05% decrease in THD_v of UPQC-CSI.

6.7 Conclusion

The proposed methodology shows the preferred introduction over produce most limit power yield appeared differently in relation to P&O and InC methodologies. The PV dealt with UPQCs are liable for the fast and exact making of implanting voltage and injects it into the structure for compensation of supply voltage agitating impacts, for instance, voltage swells. The obtained reproduction results show that UPQC with ZSI implants the reasonable proportion of three-stage mixing voltage stood out from UPQC with VSI and CSI. The reenactment results moreover exhibit that the proposed

UPQC-ZSI shows a preferable capacity over annihilating the source current and load voltage harmonic stood out from UPQC-VSI and UPQC-CSI.

References

- Ahmed J, Salam Z (2015) An improved perturb and observe (P & O) maximum power point tracking (MPPT) algorithm for higher efficiency. *Appl Energy* 150:97–108
- Ahmed J, Salam Z (2016) A modified P&O maximum power point tracking method with reduced steady state oscillation and improved tracking efficiency. *IEEE Trans Sustain Energy* 7:1506–1515
- Alam MR, Muttaqi KM, Bouzardoum A (2015) Characterizing voltage sags and swells using three-phase voltage Ellipse parameters. *IEEE Trans Indus Appl* 51:2780–2790. <https://doi.org/10.1109/TIA.2015.2397176>
- Ali US (2018) Impedance source converter for photovoltaic stand-alone system with vanadium redox flow battery storage. *Mater Today Proc* 5:241–247
- Alik R, Jusoh A (2018) An enhanced P&O checking algorithm MPPT for high tracking efficiency of partially shaded PV module. *Sol Energy* 163:570–580
- Balamurugan M, Sivakumaran TS, Devi MA (2013) Voltage sag/swell compensation using Z-source inverter DVR based on FUZZY Controller. *IEEE International Conference on Emerging Trends in Computing, Communication and Nanotechnology (ICECCN)*, 648–653
- Carrasco M, Mancilla-David F (2016) Maximum power point tracking algorithms for single-stage photovoltaic power plants under time-varying reactive power injection. *Sol Energy* 132:321–331
- Farhat M, Barambones O, Sbita L (2015) Efficiency optimization of a DSP-based standalone PV system using a stable single input fuzzy logic controller. *Renew Sustain Energy Rev* 49:907–920. <https://doi.org/10.1016/j.rser.2015.04.123>
- Fathabadi H (2016) Novel fast dynamic MPPT (maximum power point tracking) technique with the capability of very high accurate power tracking. *Energy* 94:466–475
- Gheibi A, Mohammadi SMA, Farsangi MM (2016) A proposed maximum power point tracking by using adaptive fuzzy logic engineering and electrical engineering 23:1272–1281
- Hanif M, Basu M, Gaughan K (2011) Understanding the operation of a Z-source inverter for photovoltaic application with a design example. *IET Power Electron* 4:278–287
- Kandemir E, Cetin NS, Borekci S (2017) A comprehensive overview of maximum power extraction methods for PV systems. *Renew Sustain Energy Rev* 78:93–112
- Kannan SA, Rakesh R, Amal MR, Kamala DV (2014) Performance analysis of PV single phase Z-source inverter. *Int J Innovative Res Electr Electron. Instrum Control Eng* 2:1069–1075
- Kermadi M, Berkouk EM (2017) Artificial intelligence-based maximum power point tracking controllers for photovoltaic systems: comparative study. *Renew Sustain Energy Rev* 69:369–386. <https://doi.org/10.1016/j.rser.2016.11.125>
- Messalti S, Harrag AG (2015) A new neural networks MPPT controller for PV systems. *IEEE International Conference on Renewable. Energy Congress*, 1–6. <https://doi.org/10.1109/IREC.2015.7110907>
- Pilehvar MS, Mardaneh RM, A (2015) An analysis on the main formulas of Z-source inverter. *Scientia Iranica Transactions d: Computer Science & Engineering and Electrical Engineering* 22(3):1077–1084
- Rahman SA, Janakiraman PA, Somasundaram P (2015) Voltage sag and swell mitigation based on modulated carrier PWM. *Electr Power Energy Syst* 66:78–85. <https://doi.org/10.1016/j.ijepes.2014.09.017>
- Reisi AR, Moradi MH, Showkati H (2013) Combined photovoltaic and unified power quality controller to improve power quality. *Sol Energy* 88:154–162

- Sadigh AK, Smedley KM (2016) Fast and precise voltage sag detection method for dynamic voltage restorer (DVR) application. *Electric Power Systems Research* 130:192–207. <https://doi.org/10.1016/j.epsr.2015.08.002>
- Saravanan V, Ramanujam R, Arumugam M (2015) Novel improved three level Z-source inverter. *Aust J Electr Electron Eng* 12:133–140
- Sundarabalan CK, Selvi K (2015) Compensation of voltage disturbances using PEMFC supported dynamic voltage restorer. *Electr Power Energy Syst* 71:77–92. <https://doi.org/10.1016/j.ijepes.2015.02.032>
- Tajuddin MFN, Arif MS, Ayob SM, Salam Z (2015a) Perturbative methods for maximum power point tracking (MPPT) of photovoltaic (PV) systems: a review. *Int J Energy Res* 39(9):1153–1178
- Tajuddin MFN, Ismail B, Azmi A, Ayob SM, Salam Z (2015b) Single phase Z-source inverter with differential evolution (DE) based maximum power point tracker. *TELKOMNIKA Indonesian J Electr Eng* 14:80–89
- Tang Y, Xie S, Zhang C (2011) An improved Z-source inverter. *IEEE Trans Power Electron* 26:3865–3868
- Tey KS, Mekhilef S (2014) Modified incremental conductance MPPT algorithm to mitigate inaccurate responses under fast-changing solar irradiation level. *Solar Energy* 101:333–342. <https://doi.org/10.1016/j.solener.2014.01.003>
- Umarani D, Seyezhai R (2016) Modeling and control of quasi z-source cascaded h-bridge multilevel inverter for grid connected photovoltaic systems. *Energy Procedia* 90:250–259
- Venkatesh C, Siva Sarma DVSS, Sydulu M (2011) Mitigation of voltage sag/swell using peak detector based pulse width modulation switched autotransformer. *Electric Power Compon Syst* 39:1117–1133. <https://doi.org/10.1080/15325008.2011.559188>
- Vodapalli P, Reddy TRS, Kalyani ST (2015) A new unified power quality conditioner for grid integration of PV system and power quality improvement feature distribution system. *IEEE International Conference on Electrical, Electronics, Signals, Communication and Optimization EESCO*
- Wu JC, Jou HL, Tsai JH (2017) A flexible grid interface for a PV power system. *Sol Energy* 144:540–547
- Yunfei XU, Xiao X, Sun T, Long Y (2016) Voltage swell compensation strategy for unified power quality conditioner with simultaneous reactive power injection. *Int J mod Power Syst Clean Energy* 4(1):113–122
- Zope PH, Somkuwar A (2012) Design and Simualtion of single-phase Z-source inverter for utility interface. *Int J Electr Eng Technol* 1:127–143